International Conference on Military Technologies 2019 (ICMT'19)
May 30 – 31, 2019, Brno, Czech Republic

UAV Range Measurement by Impulse Laser Rangefinder

Teodor Balaz, Jaroslav Krejci, Miroslav Svec and Martin Drahansky
University of Defence, Kounicova 65, 662 10 Brno, Czech Republic,
teodor.balaz@unob.cz, jaroslav.krejci@unob.cz, miroslav.svec@unob.cz
Brno University of Technology, Antoninska 548/1, 601 90 Brno, drahan@fit.vutbr.cz

***Abstract*—In this paper we present result and analysis of a UAV range measurement modeling. The statistical apparatus, used in this paper, corresponds to a specific pre-selected example of a moving UAV with specified flight elements. We have focused on achieving a qualitative evaluation of impulse lase rangefinder (ILR) frequency. The frequency evaluation is based on modeling of the probability of distance measurement depending on the UAV distance.**

Keywords; rangefinder; simulatin; modeling; UAV range

I. INTRODUCTION

Novadays, there is wide use of small unmanned aerial vehicles (UAV) wide spectrum of areas. Their low cost, flexibility of use, low service cost and independence on infrastructure make them ideal carriers of physical measurement and capturing systems. On the other hand, due to their properties and easy availability they pose considerable high security risk. To problematic of defense and area protection is given high attention in all technologically advanced countries. UAV-interceptors shooting nets from close proximity are deployed against UAV's, systems that will take over the control of the UAV, theories that consider weapon systems with focusing high energy beams are developed. Among curiosities in this area is for example training of bird predators to intercept UAV.

UAV has regularly small dimensions and its reflective area is very small. To achieve low weight of UAV it is often constructed using carbon composite materials which have low reflectance. Furthermore, UAV's have high maneuverability. That contributes to technical problems when completing firing objective.

Incapacitation of UAV has to be done in several consecutive phases. UAV has to be recognized, identified, localized and then the UAV flight parameters are determined. Based on the accepted UAV movement hypothesis the interception of the projectile with the UAV task is solved for given weapon system. Setting of the lead angle on the weapon system follows in such a way that the fire mission UAV incapacitation is completed.

Each of these phases of UAV incapacitation poses difficult problem.

We assume to create set of articles dealing with problematic of UAV recognition [1], measurement of its range, UAV hit probability by automatic weapons and finally organization of attack on UAV.

II. UAV COORDINATES ANALYSIS

The first theoretical problem that we solved was modeling of small UAV range measurement by ILR. After statistical analysis of numerical experiment of UAV range measurement, we conducted field experiment to verify solutions of statistical analysis for several predefined ranges. UAV range estimation by ILR model calculations were computed by ILD.EXE computer program [2]. Statistical analysis was calculated from set of 500 values for each range. The assumption was that measurements were conducted by ten independent ILR of same type and there were fifty measurements for each range by each ILR. In mathematical model of ILR the radiated power of the impulse was adjusted in range $P \in \langle 0.1 \div 2 \rangle$ MW. Entrance pupil of the receiving objective optical set has diameter of $D_{VP} = 100$ mm. In ILR receiver we assume use of avalanche photodiode InGaAs with sensitivity of $k_{pld} = 0.65$A/W, with threshold current i_k = 120 nA and noise gain is $\sigma_{in} = 20$ nA (Figure 1). Range of the ILR is dependent also on the divergence of the optical beam [3]. With high quality rangefinders the divergence value reaches $2\theta = 0.4$ mrad for intensity of 1/e. Greater ranges can be achieved with such small divergence, but we assume, that the non-cooperating target is sufficiently large and with smaller targets the ILR has to be focused very precisely. Precise aim is hard to achieve with small area [4] targets so we calculated with laser beam divergence of $2\theta = 1$ mrad. Mean rectification error of the ILR was set for both angle of elevation and angle of aim to $E_\varphi = E_\psi = 0.1$ mrad. Aim deviation mean square root for both angle of elevation and angle of aim was set to $\sigma_\varphi = \sigma_\psi = 0.3$ mrad. Drone as a target was replaced by rectangle with width of $a = 0.5$ m and height of $b = 0.1$ m. Its reflectance was $\rho_1 = 0.1$ m in case that the drone is manufactured from carbon fiber composites without protective paint. In case of use of black protective paint, the reflectance was set to $\rho_2 = 0.25$ m. Damping of laser beam in atmosphere was calculated for visibility of four kilometers [5].

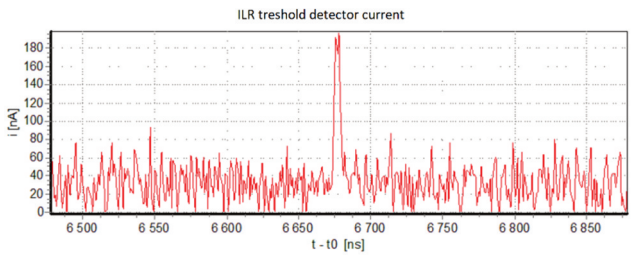

Figure 1. Simulation of current on the detector of receiving ILR diode.

In the Fig. 2, there is spatial arrangement to determine given parameters of UAV flight. Origin of the coordinate system is at the observers post (weapon post). Horizontal plane A_0OC_0, in which lays the origin is the instrument plane. UAV is observed in the point A, in which its height is h_A, slant range is s_A, and horizontal range is s_{A0}. The shortest slant range to UAV is in the point B, then the distance of points $\overline{OB_0} = P$ is Closest Point of Approach of drone.

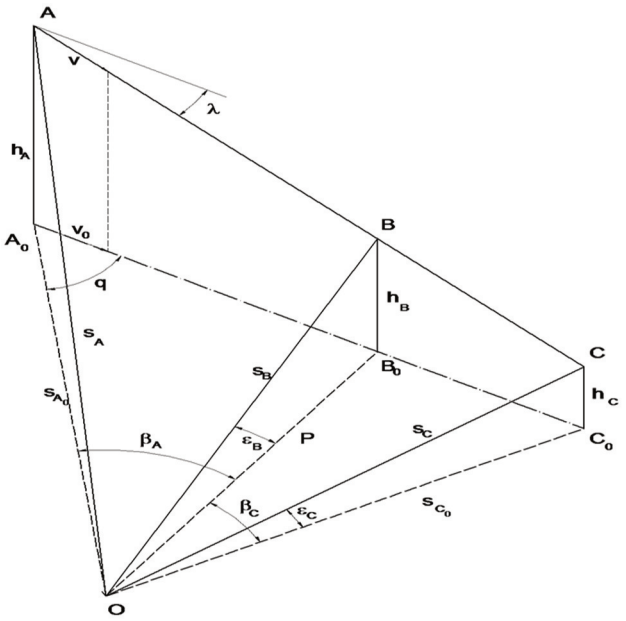

O – weapon post, P – flight parameter of target, λ – angle of decent, ε – angle of elevation of the target, h –height of the target, β – target azimuth, q –angle of target orientation, s_A-slant range of the target in point A, s_{A0} –horizontal range of the target

Figure 2. Parameters of movement of low flying target.

For horizontal velocity of the target it is true that:

$$v_0 = v \cdot \cos\lambda. \tag{1}$$

Immediate height of the target is given by formula:

$$h = h_p - v_0 \cdot \mathrm{tg}\,\lambda. \tag{2}$$

For horizontal velocity of the target it is true that:

$$s_{d_0} = \sqrt{(v_0 \cdot t)^2 \cdot p^2} s_{d_0} = \sqrt{(v_0 \cdot t)^2 \cdot p^2}. \tag{3}$$

Angle of elevation of the target ε and angular speed of elevation ω_ε are given by formula:

$$\varepsilon = \arccos\left(\frac{s_{d_0}}{s_d}\right) \omega_\varepsilon = \frac{d\varepsilon}{dt}. \tag{4}$$

Azimuth of the target and azimuth angular speed of the target [6] are describe bellow:

$$\beta = \arccos\left(\frac{P}{s_d}\right), \tag{5}$$

$$\omega_\beta = \frac{d\beta}{dt} = \frac{a}{1+a^2 \cdot t^2},\ a = \frac{v}{P}, \tag{6}$$

And for azimuth acceleration of the target it is true that:

$$\frac{d^2\beta}{dt^2} = -\frac{2 \cdot a^3 \cdot t}{(1+a^2 \cdot t^2)^2}. \tag{7}$$

The maximum azimuth angular speed of the target is in moment $t = 0$, that is when the target is flying at the parameter (7).

III. UAV Distance Measurement Model

A. The Example to Clarify the Issue

UAV is flying in line at parameter $P = 100$ m, at constant velocity $v = 70\ \mathrm{m} \cdot \mathrm{s}^{-1}$, angle of descent is $\lambda = 3°$, height of UAV flight at parameter is $h_b = 200$ m. Time of observation of UAV is $t = 60$ s. Data analysis result is presented in Fig. 3, 4, 5, 6, 7, 8, 9 and 10.

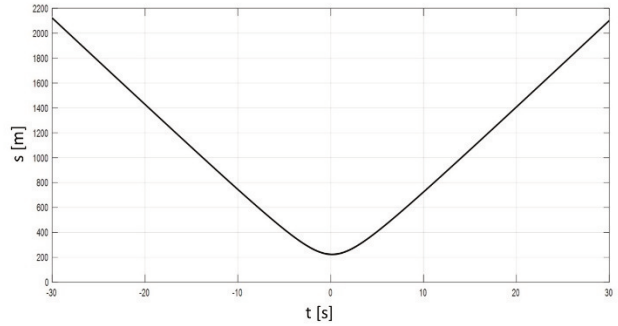

Figure 3. Dependency of slant distance of UAV on time.

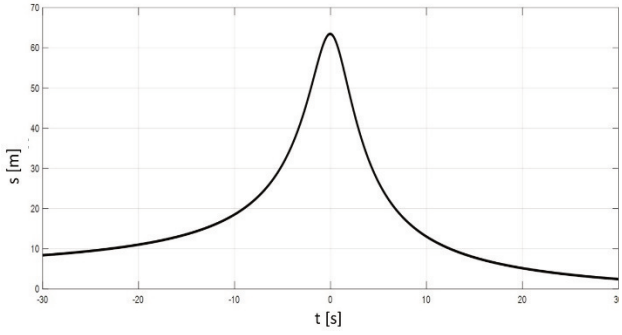

Figure 4. Dependency of angle of elevation ε on time.

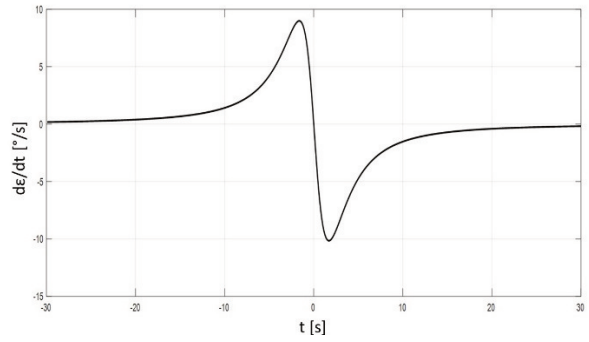

Figure 5. Dependency of position angular speed $\frac{\mathrm{d}\varepsilon}{dt}$.

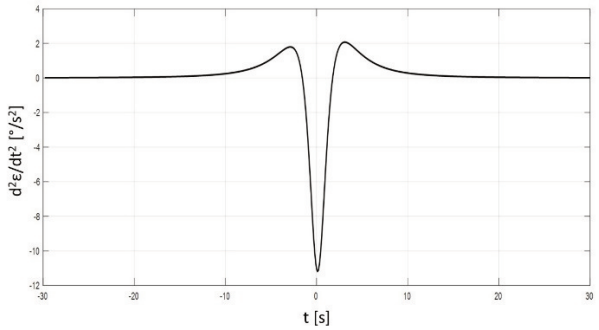

Figure 6. Dependency of acceleration $\frac{d^2\varepsilon}{dt^2}$ on time.

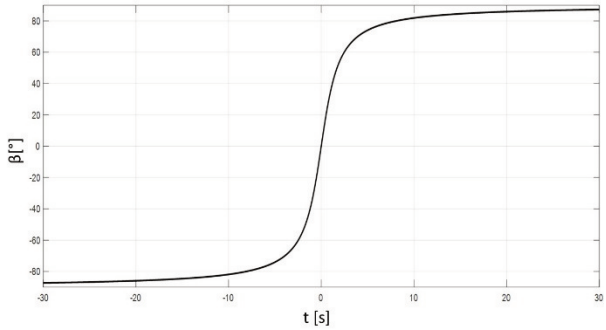

Figure 7. Dependency of horizontal angle of UAV β on time.

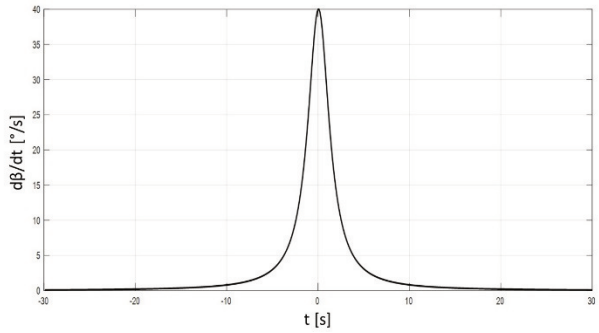

Figure 8. Dependency of horizontal angular speed $\frac{\mathrm{d}\beta}{dt}$ on time.

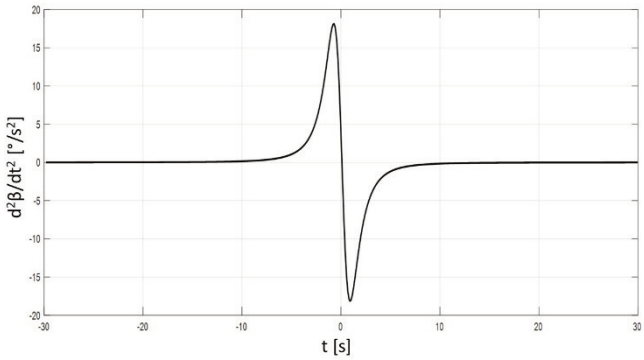

Figure 9. Dependency of acceleration $\frac{\mathrm{d}^2\beta}{dt^2}$ on time.

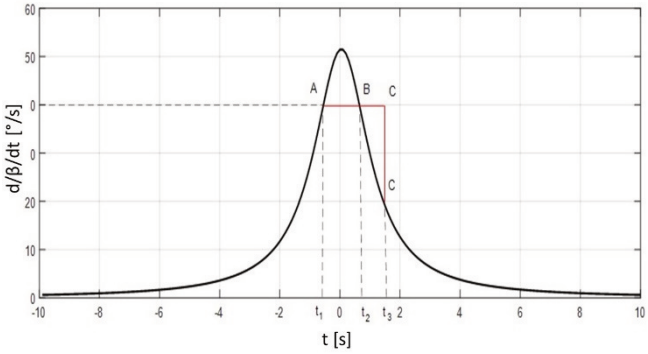

Figure 10. Dependency of angle of elevation ε on time.

Calculations of individual simulations were performed. Results of simulation of UAV range measurement by ILR represent Tab. 1, Tab. 2 and Tab. 3.

TABLE I. RESULTS OF SIMULATION OF UAV RANGE MEASUREMENT

	$P = 1.5$ MW $\rho = 0.1$							
d [m]	600	700	800	900	1000	1100	1200	1300
n	350	328	251	185	92	36	23	12
$d_{stř}$[m]	600.0	699.6	800.4	900.7	1002.3	1105.2	1172.1	1242.0
σ_d[m]	0.11	8.37	9.57	14.58	19.85	53.36	98.47	144.73
$Q_{1/10}$	599.9	699.9	799.9	900.1	1000.1	1100.0	985.7	1041.2
$Q_{10/10}$	600.2	700.2	800.2	900.4	1000.5	1102.7	1267.5	1389.4
f	0.7	0.656	0.502	0.37	0.184	0.072	0.046	0.024

Tab. I represents the results of simulation of UAV range measurement by ILR with power of the impulse $P = 1.5$ MW, reflectance of the target $\rho = 0.1$.

TABLE II. RESULTS OF SIMULATION OF UAV RANGE MEASUREMENT

	$P = 1.5$ MW $\rho = 0.25$											
d [m]	600	700	800	900	1000	1100	1200	1300	1400	1500	1600	1700
n	434	401	394	364	315	303	228	210	123	61	16	13
$d_{stř}$[m]	600.5	701.1	799.9	900.4	1000	1101.8	1197.5	1298	1394	1506	1613	1711
σ_d[m]	8.69	12.28	0.09	5.88	8.86	14.29	23.15	27.95	37.50	62.91	115.8	130.1
$Q_{1/10}$	599.8	699.8	799.8	899.9	999.9	1099.9	1200.1	1300	1400	1500	1429	1510
$Q_{10/10}$	600.0	700.0	800.0	900.2	1000	1100.1	1200.3	1300	1400	1500	1702	1858
f	0.868	0.802	0.788	0.728	0.63	0.606	0.456	0.42	0.246	0.122	0.032	0.026

Tab. II represent the results of simulation of UAV range measurement by ILR with power of the impulse $P = 1.5$ MW, reflectance of the target $\rho = 0.25$.

TABLE III. RESULTS OF SIMULATION OF UAV RANGE MEASUREMENT

	P = 2 MW, $\rho = 0.25$							
d [m]	600	700	800	900	1000	1100	1200	1300
n	439	433	390	368	345	317	309	253
$d_{stř}$[m]	599.9	699.9	799.8	900.4	1000.2	1100.4	1200.0	1297.7
σ_d[m]	6.72	1.53	6.52	13.33	9.9	9.64	5.05	20.31
$Q_{1/10}$	599.8	699.8	799.8	899.9	999.9	1099.9	1200.0	1300.0
$Q_{10/10}$	600.0	699.9	799.9	900.1	1000.1	1100.1	1200.2	1300.2
f	0.878	0.866	0.78	0.736	0.69	0.634	0.618	0.506
d [m]	1400	1500	1600	1700	1800	1900	2000	
n	213	163	74	58	22	15	14	
$d_{stř}$[m]	1398.9	1505.6	1606.9	1710.2	1826.7	2000.2	2038.9	
σ_d[m]	17.80	32.82	51.36	39.94	132.1	151.1	210.8	
$Q_{1/10}$	1399.9	1500.1	1600.1	1700.02	1655.6	1900.1	1686.8	
$Q_{10/10}$	1400.3	1500.5	1600.5	1700.57	2029.2	2237.2	2331.0	
f	0.426	0.326	0.148	0.116	0.044	0.03	0.028	

Tab. III represents the results of simulation of UAV range measurement by ILR with power of the impulse P = 2 MW, reflectance of the target $\rho = 0.25$.

The following parameters are listed on the tables above: $d\,[m]$ actual range to target, n number of detected ranges, $d_{stř}[m]$ selection average of target ranges, σ_d[m] selection standard deviation, $Q_{1/10}$ lower decile, $Q_{10/10}$ upper decile.

B. *Statistic Analysis of Measurement Frequency*

To determine the probability of distance measurement the following statistical characteristics have been identified. Dependency of frequency of detection of target range f on its range for ILR with power of the impulse $P = 1.5$ MW, reflectance of the target $\rho = 0.25$, represents in Fig. 11.

$$f = \sum_{i=0}^{2} a_i \cdot d^i, a = \{1.046, -7.97 \cdot 10^{-5}, -3.309 \cdot 10^{-7}\}. \quad (8)$$

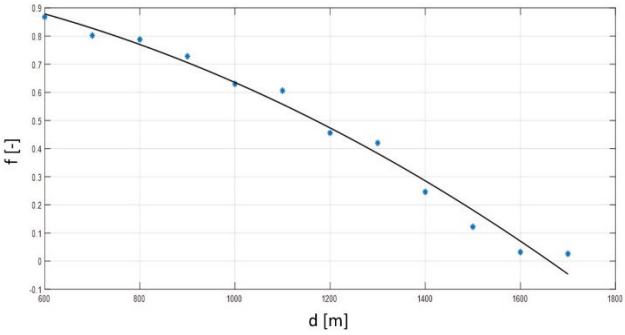

Figure 11. Dependency of frequency of detection of target range.

Figure 12 represented the dependency of selection standard deviation σ_d on range of the target for ILR with power of the impulse $P = 1.5$ MW, reflectance of the target $\rho = 0.25$, where

$$\sigma_d = 0.2581 \cdot e^{3{,}699 \cdot 10^{-3} \cdot d}. \quad (9)$$

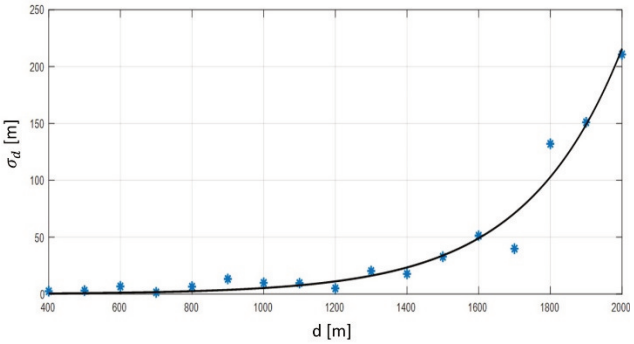

Figure 12. Dependency of selection standard deviation σ_d on range of the target.

Dependency of frequency of detection of target range f on its range for ILR with power of the impulse $P = 2$ MW, reflectance of the target $\rho = 0.25$ represents Fig. 13.

$$f = \sum_{i=0}^{2} a_{i+1} . d^i, a = \{0.9569 \;\; 5.384 \cdot 10^{-5}, \; -2.806 \cdot 10^{-7}\}. \quad (10)$$

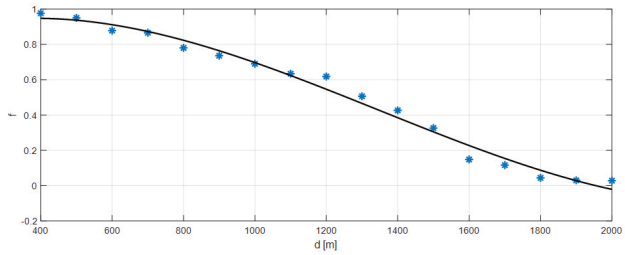

Figure 13. Dependency of frequency of detection of target range.

Figure 14 represents Dependency of selection standard deviation σ_d on range of the target for ILR with power of the impulse $P = 2$ MW, reflectance of the target $\rho = 0.25$, where

$$\sigma_d = 0{,}07947 \cdot e^{3{,}877 \cdot 10^{-3} \cdot d}. \quad (11)$$

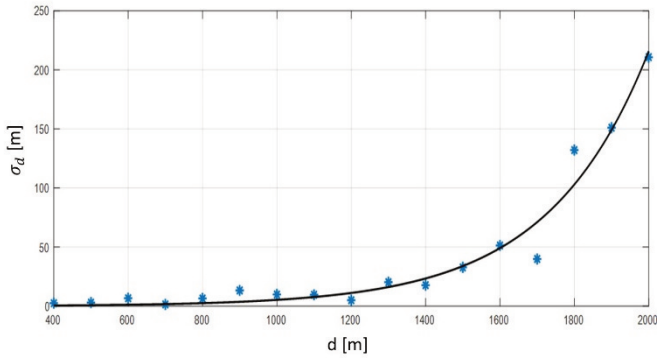

Figure 14. Dependency of selection standard deviation σ_d on range of the target.

When there is sufficiently high number of attempts N and frequency f is not near 0 or 1, the frequency distribution can be considered as a normal distribution. Because of that, the method to determine probability integral is the same as integral for mean value. Peculiarity is it, that root mean error of frequency f for $0 < f < 1$ has value

$$\overline{\sigma_p} = \sqrt{\frac{f \cdot (1-f)}{N}}, \tag{12}$$

that correspond with

$$P_{(\bar{X}-\varepsilon \le m_x \le \bar{X}+\varepsilon)} = \Phi_{(\beta)} = \beta\ , \quad \frac{\varepsilon}{\bar{\sigma}} = \Phi^{-1}_{(\beta)}\ , \tag{13}$$

where Φ is Laplace integral [6]

$$\Phi(y) = \frac{2}{\sqrt{2\pi}} \cdot \int_0^y \mathrm{e}^{-\frac{t^2}{2}} \cdot \mathrm{d}t = \mathrm{erf}\left(\frac{y}{\sqrt{2}}\right), \tag{14}$$

$$\mathrm{erf}(z) = \frac{2}{\sqrt{\pi}} \cdot \int_0^z \mathrm{e}^{-t^2} \cdot \mathrm{d}t. \tag{15}$$

For calculation of values of function $\mathrm{erf}(z)$ we will use following mathematical development [7]:

$$\mathrm{erf}(z) = \frac{2}{\sqrt{\pi}} \cdot \int_0^z \mathrm{e}^{-t^2} \cdot \mathrm{d}t =$$

$$\frac{2z}{\sqrt{z}} \cdot \left[1 - \frac{z^2}{1!\cdot 3} + \frac{z^4}{2!\cdot 5} - \frac{z^6}{3!\cdot 7} + \frac{z^8}{4!\cdot 9} - \ldots\right]. \tag{16}$$

This way of determining the probability integral can be used to calculate inverse task, which often occurs when planning experiments. For example, how many UAV range measurements is needed to obtain mean range value or frequency of the random phenomenon that have given value of probability integral? For number of repetitions n:

$$\mathrm{n} = \left[\frac{\sigma}{\Delta} \cdot \Phi^{-1}_{(\beta)}\right]^2. \tag{17}$$

Inverse Laplace function $\Phi^{-1}_{(\beta)}$ for calculation of probability integral [8]:

$$\Phi^{-1}_{(\beta)} = 0.1994 \cdot e^{(2.308 \cdot \beta)} +$$

$$+ 5.354 \cdot 10^{-15} \cdot \mathrm{e}^{(32.78 \cdot \beta)} \ \wedge \beta \in (0.3 \div 1\rangle. \tag{18}$$

Dependency of number of target range measurements on distance of the target with probability of measuring the correct value $\beta = 0.85$ for ILR with power of the impulse $P = 1.5\ MW$, reflectance of the target $\rho = 0.25$, error of the measurement $\Delta = 15\ m$ represents Fig. 15.

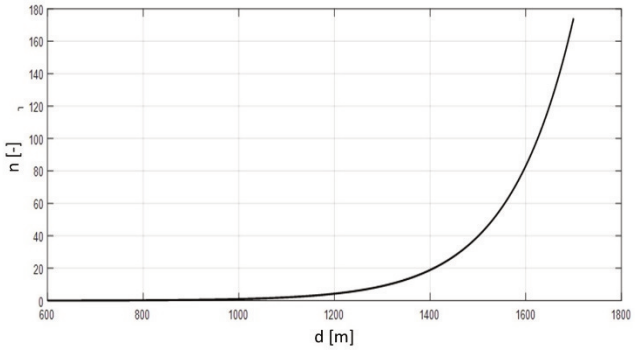

Figure 15. Dependency of number of target range measurements on distance of the target.

Dependency of number of target range measurements on distance of the target with probability of measuring the correct value $\beta = 0.85$ for ILR with power of the impulse $P = 2$ MW, reflectance of the target $\rho = 0.25$, error of the measurement $\Delta = 15\ m$ represents Fig. 16.

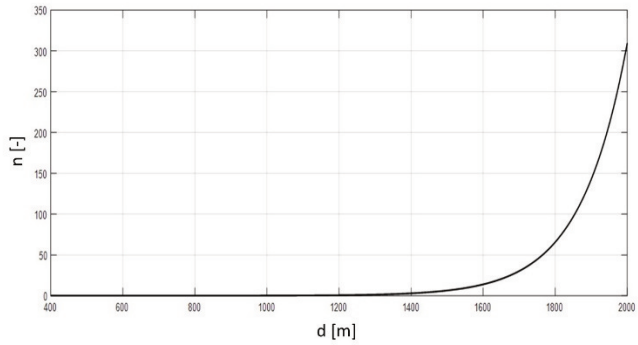

Figure 16. Dependency of number of target range measurements on distance of the target.

As we can see from results of statistical analysis of simulations of UAV range measurement by ILR, to determine correct UAV range with defined probability β and acceptable error Δ, more measurements would need to be conducted. Predicted velocity of the UAV in tens of meters per second, causes considerable big difference in position relative to the observer (Fig. 17).

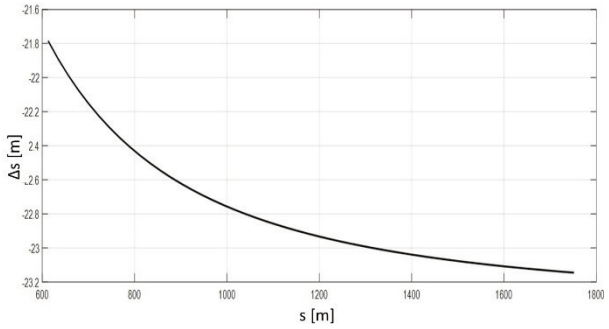

Figure 17. Dependence of range ΔS on UAV range for frequency of three measurements per second.

With repetitive measurement, the probability of correct UAV range detection changes with the change of UAV position change as is shown in Fig. 9 and Fig. 11. Total probability of target range measurement P_m after n measurements assuming that P_{d_i} is probability of range measurement in distance d_i is given by formula:

$$\mathrm{P_m} = 1\text{-}\prod_{\mathrm{i=1}}^{\mathrm{n}}(1\text{-}\mathrm{P_{d_i}}). \tag{19}$$

In the following (Fig. 18, 19) there are shown probabilities of range measurements P_m by ILR with power of the impulse $P = 2$ MW depending on UAV range for three and five measurements per second. In each series the range was measured 2 times (blue line), 3 times (red line) and 5times (black line).

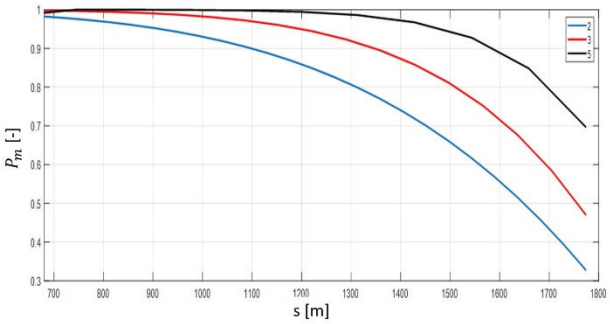

Figure 18. Probability of range measurement P_m by ILR depending on UAV range for frequency of three measurements per second.

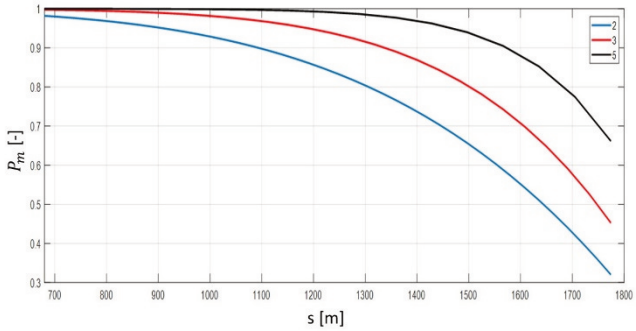

Figure 19. Probability of range measurement P_m by ILR depending on UAV range for frequency of five measurements per second.

From evaluation of range measurement by ILR probabilities P_m depending on UAV range with frequency of three and five measurements per second we can say, that three measurements in one session are sufficient to determine UAV range with sufficient precision.

IV. Conclusion

Identification, localization and determination of movement parameters of UAV are the basic predispositions to determine point of impact of UAV and projectile, which leads to successful completion of fire task, incapacitation of UAV repeatedly measuring the distance of a flying UAV is necessary to locate and detect movement of UAV parameters. Results of repeated UAV range measurement modeling imply, that it is a difficult problem. UAV range is amongst the most significant variable parameters when determining the point of impact. Significance of knowledge of exact UAV range increases with UAV range to weapon system. It is given by decreasing precision and probability of measurement with ILR, precision of aim of weapon system to determined direction in given time, but also by increased bullet spread and that the bullet time of flight is determined with certain precision.

To achieve greater UAV hit probability it is required from weapon system to have higher bullet velocity. With increasing bullet velocity, the UAV incapacitation task becomes easier. However, the bullet velocity can´t be increased indefinitely. If the weapon system doesn't use kinetic energy of bullets or its shrapnel, but focused electromagnetic energy of for example high powered laser beam instead, it would lead to significant simplification. Weapon system targeting system wouldn't have to solve the task of finding the UAV and projectile point of impact based on UAV movement hypothesis and delay between firing of a bullet and its target impact, but it would be sufficient o follow the UAV with sufficient precision and the delay would be from technical standpoint zero.

References

[1] Racek, František; Barta, Vojtěch. Spectrally Based Method of Target Detection in Acquisition System of General Fire Control System. In: *Conference Proceedings of* ICMT'17. Piscataway, NJ 08854-4141 USA: Institute of Electrical and Electronics Engineers Inc., 2017, p. 22-26. ISBN 978-1-5386-1988-9.

[2] V.Cech, J. Jevicky. OPROX software, Projekt CILEPAS. *CILEPAC 1.0.8*. ČR. (2008). www.oprox.cz

[3] Willers, Cornelius J. Electro-Optical System and Design: A radiometry Perspective. Bellingham, Washington: SPIE Press, 2013. ISBN 978-0-8194-9569-3.

[4] J. Balla, Z. Krist, F. Racek, P. Melsa, V. Neuman, C. I. LE. Analysis and Parameter Identification of Automatic Cannon Carriages. Defence Science Jurnal, 2018, vol. 68, no. 6, p. 525-532. ISSN 0011-748X. DOI: 10.14429/dsj.68.12395.

[5] Horak, Richard. Physical basics of laser rangefinders and gyroscopes. Olomouc: Chlup.net, 2012. ISBN 978-80-903958-6-2.

[6] Balaz, Teodor. Possibilities of using passive optoelectronic rangefinder in current fire control systems of tanks and BMP. Brno, 2003. Habilitation work. Military Academy in Brno, Faculty of Military Engineering,, Department of Weapon Systems

[7] Bronshtein, I.N., K.A. K.A. Semendyaev, G. Musiol a H. H.Muehlig. Handbook of Mathematics. 5 th Ed. Berlin, Heidelberg: Springer-Verlag, 2007. ISBN 978-3-540-72121-5.

[8] Korn, Granino a Theresa Korn. Mathematical Handbook: For scientists and engineers. 2 nd, enlargend and revised edition. McGraw-Hill: McGraw-Hill Book Company, 1968.